Spin-dependent tunnelling through epitaxial GaAs(001) and (110) barriers

2004 J. Phys.: Condens. Matter 16 S5823

(http://iopscience.iop.org/0953-8984/16/48/057)

INSTITUTE OF PHYSICS PUBLISHING JOURNAL OF PHYSICS: CONDENSED MATTER

J. Phys.: Condens. Matter **16** (2004) S5823–S5832 PII: S0953-8984(04)79274-7

Spin-dependent tunnelling through epitaxial GaAs(001) and (110) barriers

Marcus Zenger, Juergen Moser, Stephan Kreuzer, Werner Wegscheider and Dieter Weiss

Institut für Experimentelle und Angewandte Physik, Universität Regensburg, 93040 Regensburg, Germany

Received 15 April 2004
Published 19 November 2004
Online at stacks.iop.org/JPhysCM/16/S5823
doi:10.1088/0953-8984/16/48/057

Abstract

We investigate transport through 5–10 nm thin epitaxial GaAs(001) and (110) barriers sandwiched between polycrystalline iron films. It turns out that tunnelling is the dominant transport mechanism; this is indicated by a nonlinear I–V-characteristic, an exponential dependence of the tunnelling current on the barrier thickness and the temperature dependence of the current. We observe a pronounced tunnelling magnetoresistance (TMR) effect at low magnetic fields. Annealing decreases the TMR effect drastically and indicates the sensitivity of this effect to layer intermixing. At high magnetic fields we observe a distinct negative magnetoresistance (MR) at low temperatures and a positive MR at higher temperatures. This negative MR contribution is only observed for ferromagnetic iron contacts and is absent if iron is replaced by copper or gold electrodes.

1. Introduction

The tunnelling magnetoresistance (TMR) effect is widely studied due to potential applications in sensors and data storage devices [1]. Up to now, most studies have been performed on magnetic tunnel junctions with a layer of amorphous alumina as insulating barrier sandwiched between two ferromagnetic electrodes [2]. A TMR of 60% at room temperature was reported by Tsunoda *et al* [3]. Nevertheless, as the basic mechanisms are still under debate, the TMR is a subject of current basic research. Theoretical models taking into account the complex band structure are based on single-crystal barriers and contacts. First-principles calculations with GaAs and ZnSe barriers predicted large magnetoresistance effects up to 100% which, in addition, depend on the barrier thickness [4, 5]. These large values have not yet been obtained in experiment [6, 7]. Tunnelling experiments employing semiconductor barriers are also relevant for the problem of spin injection into semiconductors [8]. Such tunnelling experiments provide an upper estimate of the spin-injection rate and therefore the maximum achievable spin polarization in a transport experiment.

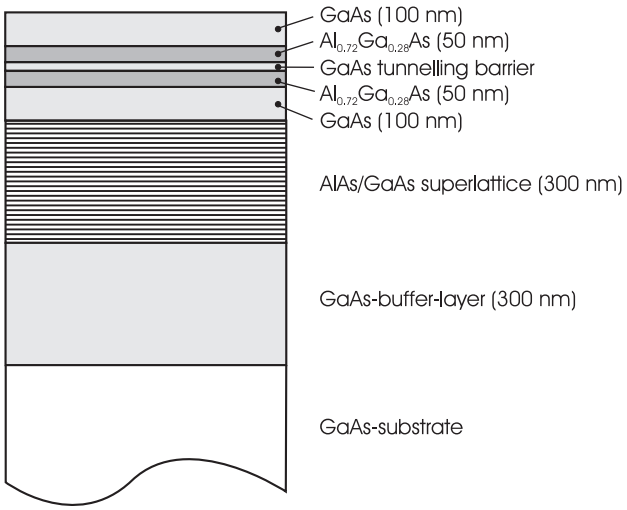

Figure 1. Semiconductor heterostructure for the preparation of the tunnel junctions. The tunnel barrier is sandwiched between two 50 nm $Al_{0.72}Ga_{0.28}As$ films and 100 nm GaAs. The 300 nm thick AlAs/GaAs superlattice acts as an etch stop layer.

2. Sample preparation

In order to realize a transport experiment through an epitaxial GaAs barrier we used a recently developed technique employing selective etching of AlGaAs sacrificial layers and thermal evaporation of iron contacts [9, 10]. This results in a rectangular tunnelling barrier, formed by the two Schottky contacts on both sides of the barrier. This technique can, in principle, be extended to fabricate fully epitaxial systems, i.e. with epitaxial iron contacts.

To fabricate Fe/GaAs(001)/Fe or Fe/GaAs(110)/Fe tunnelling elements we start from GaAs heterostructures, grown on semi-insulating (SI) GaAs(001) or GaAs(110) wafers by molecular beam epitaxy (MBE) at a growth temperature of 630 °C. A 300 nm GaAs buffer layer is deposited first, followed by a digital superlattice consisting of 106 double layers of 0.57 nm GaAs and 2.26 nm AlAs, acting in effect as an 300 nm thick sacrificial $Al_xGa_{1-x}As$ layer with an Al content of 0.8. Finally, the 5–10 nm thick GaAs barrier is sandwiched between two 50 nm $Al_{0.72}Ga_{0.28}As$ films and 100 nm GaAs. The corresponding layer sequence is displayed in figure 1.

The sample preparation involving optical lithography is sketched in figure 2, and was described in detail previously [9]. By highly selective wet chemical etching the sacrificial layers get removed and the polycrystalline bottom contact is evaporated thermally (figure 2(a)). Then the sample is epoxy bonded upside down onto a SI GaAs(001) host substrate (figure 2(b)). The original substrate and the 300 nm thick $Al_xGa_{1-x}As$ etch stop layer are selectively removed. To get access to the bottom contact a mesa is prepared by optical lithography and wet chemical etching. The top metal contact is evaporated after selectively etching a 16 μm diameter hole into the insulating 100 nm GaAs and 50 nm $Al_xGa_{1-x}As$ (figure 2(c)). A sketch of the top view of the final structure with the 16 μm diameter tunnelling junction in the centre is shown in figure 2(d).

The measurements were carried out in a four-point technique employing an HP Semiconductor Analyzer 4155A. The samples were mounted in a variable temperature insert (VTI) of a ^{4}He cryostat with a superconducting coil. The magnetic field was aligned in the

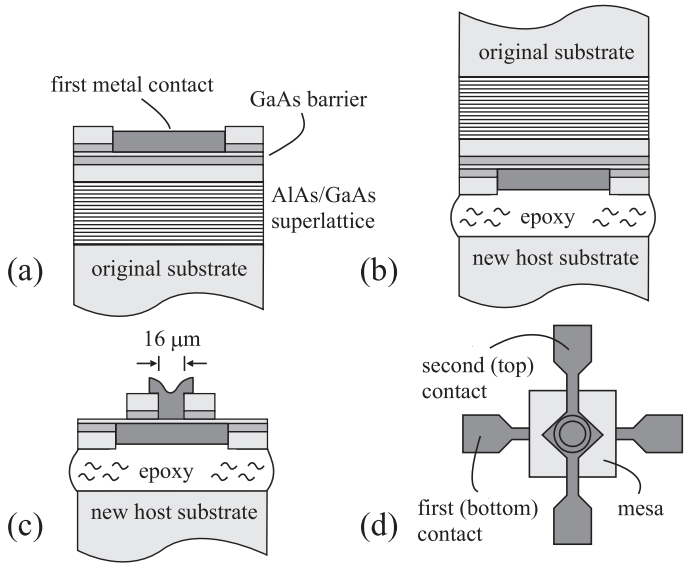

Figure 2. Preparation of magnetic tunnel junctions using the epoxy-bond-and-stop-etch (EBASE) technique: (a) after evaporating the top metal contact the sample is (b) inverted and epoxy bonded onto a SI GaAs host substrate; (c) and (d): side and top view of the completed sample.

plane of the tunnelling barrier and the temperature in the VTI was varied between 4 and 237 K in experiment.

3. Experiments and discussion

3.1. I–V measurements

Our previous and present experimental findings provided convincing evidence that quantum mechanical tunnelling is the dominating transport channel in our devices [9, 10]. In particular, the I–V-characteristic at zero magnetic field, investigated previously [10], is strongly nonlinear with a kink between 0.7 and 0.8 V (see figure 3(a)) which is ascribed to Fowler–Nordheim tunnelling (FNT). A barrier height ϕ of this size is expected from Fermi-level pinning at GaAs surfaces, which occurs at about one half of the energy gap E_g: $\phi = E_g/2 = 0.76$ eV at 0 K [10].

In addition, the tunnelling current shows an almost perfect exponential dependence on the barrier thickness d, $I \propto \exp(-2\kappa d)$ (figure 3(b)). The damping constant $\kappa = 0.9 \pm 0.1$ nm^{-1} is in close agreement with the model of Mavropoulos *et al* [11]. In the simplest approach the damping constant κ is given by $\sqrt{2m\phi}/\hbar$ with m the effective electron mass in GaAs. With this simple expression we obtain $\kappa \approx 1.15$ nm^{-1}.

In a second set of experiments we checked the temperature dependence of the tunnelling current (figure 4). The current shows a quadratic increase with increasing temperature. The inset shows the dependence of the thermal part of the current $I_{th} = I(T) - I(2.5\ \mathrm{K})$ on T^2. Such a quadratic increase is expected for the temperature dependence of the gap of GaAs, which varies quadratically from 1.52 eV at 4.2 K to 1.42 eV at room temperature [12]. The ratio $\frac{I(T)}{I(T_0)} = \frac{\phi^{\frac{1}{2}}(T)\exp(-2(2m)^{\frac{1}{2}}/\hbar \cdot \mathrm{d}\phi^{\frac{1}{2}}(T))}{\phi^{\frac{1}{2}}(T_0)\exp(-2(2m)^{\frac{1}{2}}/\hbar \cdot \mathrm{d}\phi^{\frac{1}{2}}(T_0))}$ obtained from Simmons' model for small bias voltages [13] is reproduced quantitatively correctly in experiments where we used $T_0 = 2.5$ K. Also these experiments confirm that tunnelling is the main transport channel.

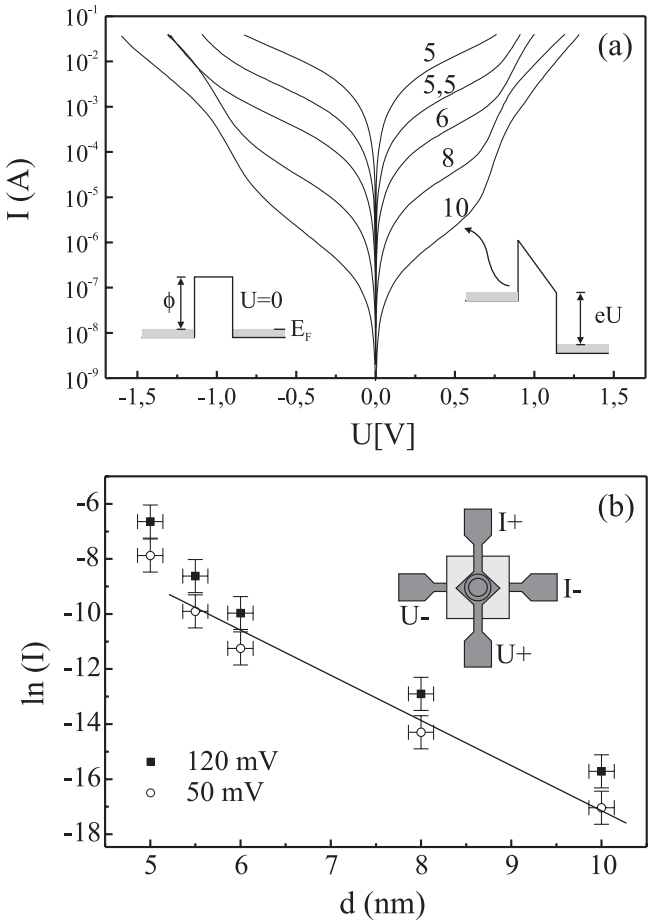

Figure 3. *I–V*-characteristics of Fe/GaAs(001)/Fe tunnel junctions at 4.2 K. (a) Dependence of current on bias voltage for samples with different barrier thickness, given in nanometres. The insets sketch the barrier at $U = 0$ and under FNT condition; (b) dependence of the tunnelling current (current in amperes) on the barrier thickness for two different bias voltages. The solid line is a guide to the eye.

3.2. Magnetoresistance measurements

In this section we now discuss tunnelling in the presence of an in-plane magnetic field. Following recent work we used iron contact layers of different thickness, 4 and 20 nm, to establish different coercive fields of the two contacts at low temperatures [10]. The TMR effect measured on a sample with 8 nm thick GaAs(001) barrier is shown in figure 5. We observe a pronounced spin-dependent resistance signal with a TMR ratio of 1.7%, which is higher by a factor eight than that previously observed [10]. Here we used the usual definition that TMR $= (R_{\uparrow\downarrow} - R_{\uparrow\uparrow})/R_{\uparrow\uparrow}$, where $R_{\uparrow\uparrow}$ ($R_{\uparrow\downarrow}$) is the resistance for parallel (antiparallel) magnetization orientation in the contacts. To estimate the degree of spin polarization of the tunnelling current we used Jullière's model [14] in which the TMR ratio is given by the spin polarization P of the density of states at the Fermi energy of the metal contacts, TMR $= 2P^2/(1 - P^2)$. A TMR effect of 1.7% corresponds to a value of about 9% for the spin polarization. We ascribe the fact that the spin polarization is significantly higher than

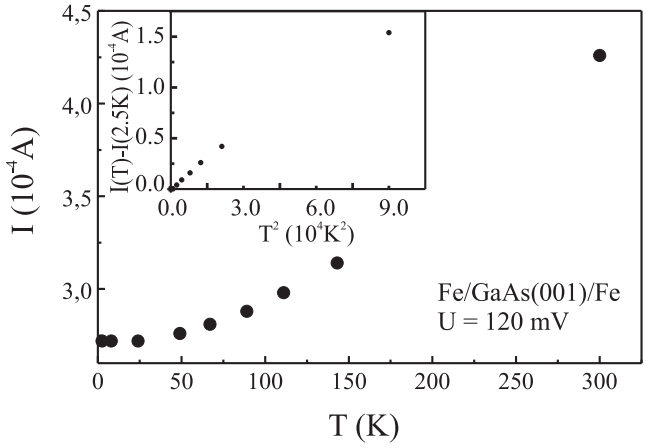

Figure 4. Temperature dependence of the tunnelling current for a Fe/GaAs(001)/Fe sample with a 6 nm thick barrier. The inset shows the dependence of the thermal part of the current $I_{\mathrm{th}} = I(T) - I(2.5\ \mathrm{K})$ on T^2.

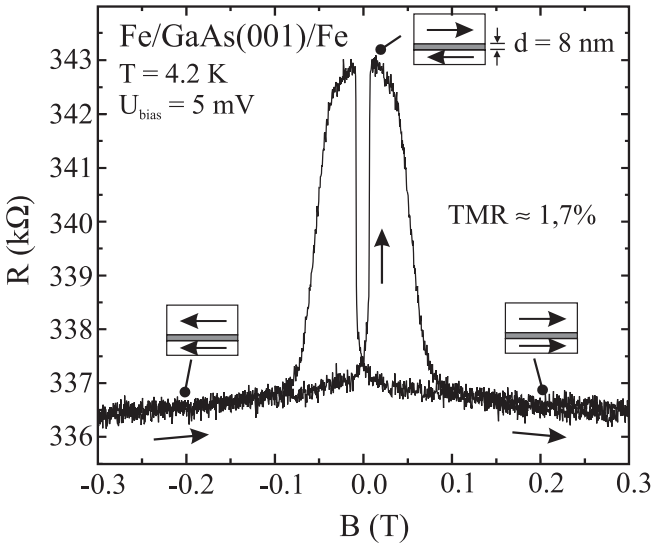

Figure 5. TMR traces of an Fe/GaAs(001)/Fe tunnel junction with a barrier thickness $d = 8$ nm measured at 4.2 K and a bias voltage of 5 mV.

previously reported [10] to new heterostructure material with reduced interface roughness and a reduction of the highest process temperature (epoxy cure) down to 80 °C. Annealing at 120 °C for 2 h decreased the TMR effect to 63% of its initial value; a second annealing step at 160 °C for 2 h decreased it to 32%; and after a last annealing step carried out at 200 °C for 2 h the TMR vanished completely. The corresponding TMR traces are displayed in figure 6. In addition, the reduction of the TMR is accompanied by a significant reduction of the resistance of the tunnelling barrier, which is only about 10% of its initial value after the three annealing steps. These experimental findings indicate the sensitivity of the TMR effect to layer intermixing or impurity diffusion.

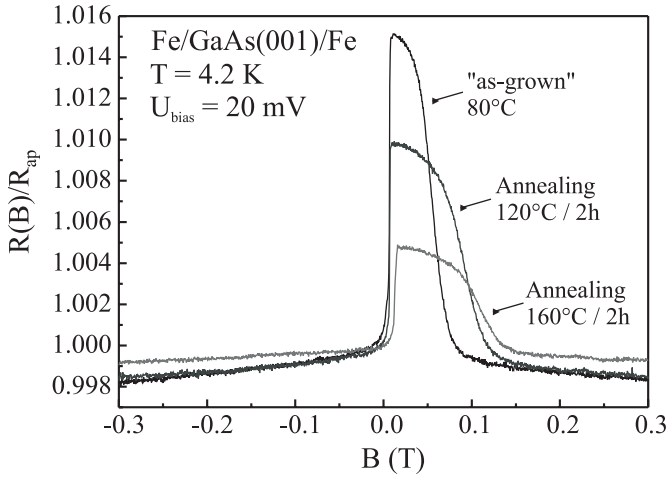

Figure 6. Magnetoresistance measurements for the same sample as in figure 5, measured at 4.2 K and a bias voltage of 20 mV. After a first annealing step (120 °C for 2 h) the TMR decreased to 63% of its initial value; after a second annealing step (160 °C for 2 h) it decreased to 32%.

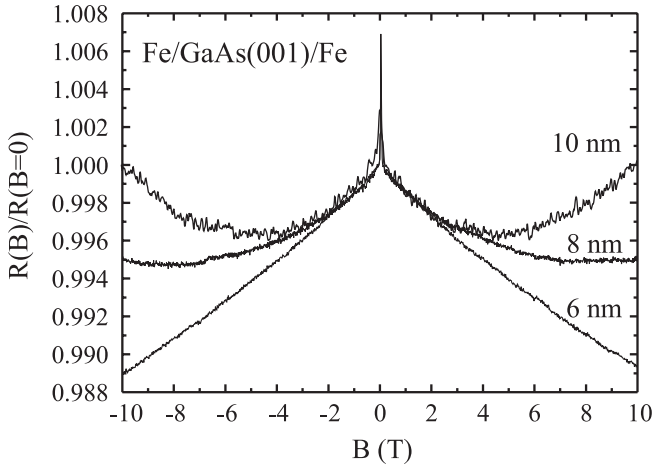

Figure 7. High-field MR measured at 4.2 K and a bias voltage of 20 mV for 6, 8 and 10 nm thin GaAs(001) barriers, sandwiched between two iron contacts. The sharp peak at $B \sim 0$ is the TMR effect.

Though our iron contacts are non-epitaxial and though we probe transport across two Fe/GaAs interfaces, our polarization values are comparable to values obtained on epitaxially grown Fe/AlGaAs LED devices [15, 16].

Figure 7 displays the high-field MR of three Fe/GaAs/Fe tunnel junctions with 6, 8 and 10 nm thick GaAs(001) barriers at 4.2 K. Their magnetic field dependence is strikingly different: while the MR for the sample with the thinnest barrier of 6 nm is negative over the investigated B-range, the MR for the thickest junction with 10 nm barrier becomes positive above ∼5 T. The spike at $B = 0$ corresponds to an antiparallel alignment of the iron contacts and is the TMR effect. The observation of a negative MR is surprising, since one expects an increasing resistance with an increasing in-plane magnetic field. In the simplest picture,

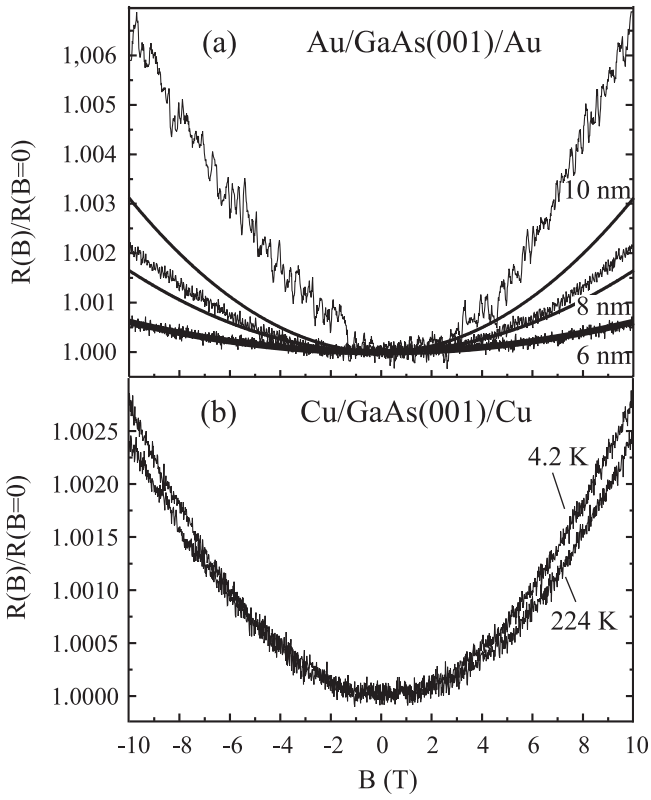

Figure 8. Tunnelling resistance of junctions with nonmagnetic contacts at 4.2 K. (a) Dependence of positive MR on barrier thickness d for Au/GaAs(001)/Au junctions. The solid curves correspond to the model of Eaves *et al* [17]. The fit to the 6 nm trace provides the parameters to calculate the magnetoresistance for the 8 and 10 nm thick barriers. (b) Temperature dependence of the normalized resistance of a Cu/GaAs(001)/Cu junction with $d = 10$ nm. The bias voltage was in both cases 20 mV.

the tunnelling electrons, moving perpendicular to the applied magnetic field, follow a curved trajectory through the barrier. The longer path in the barrier is associated with an enhanced damping of the electron wavefunction and thus an increase of the resistance. Eaves *et al* [17] obtain for the tunnel current $I(B)$ for an in-plane magnetic field the following expression: $I(B) = I_0 \exp(-\beta B^2)$ with $\beta = e^2 d^3 \kappa / 6m\phi$. Here, I_0 is the current at $B = 0$. To test this prediction and to demonstrate that the negative MR is linked to the ferromagnetism of the contacts we fabricated reference Au/GaAs(001)/Au and Cu/GaAs(001)/Cu tunnel junctions with different barrier thickness d. The nonmagnetic contacts are polycrystalline just like the Fe contacts in the ferromagnetic tunnel junctions. Corresponding data are shown in figures 8(a) and (b), respectively. As expected, the positive MR increases with increasing barrier thickness, shown in figure 8(a). Though the expression for $I(B)$ does not fit quantitatively, the dependence of $I(B)$ on the barrier thickness d is described qualitatively correctly. However, the most important observation here, displayed in figure 8(b), is that the tunnelling current is essentially independent of temperature. If we then assume that the high-field MR shown in figure 7 consists of two contributions, a temperature independent positive MR, due to the increased tunnelling path, and an unknown one, associated with the ferromagnetic contacts, we can extract the latter one. This is shown for temperature-dependent MR data in figure 9. Figure 9(a) displays

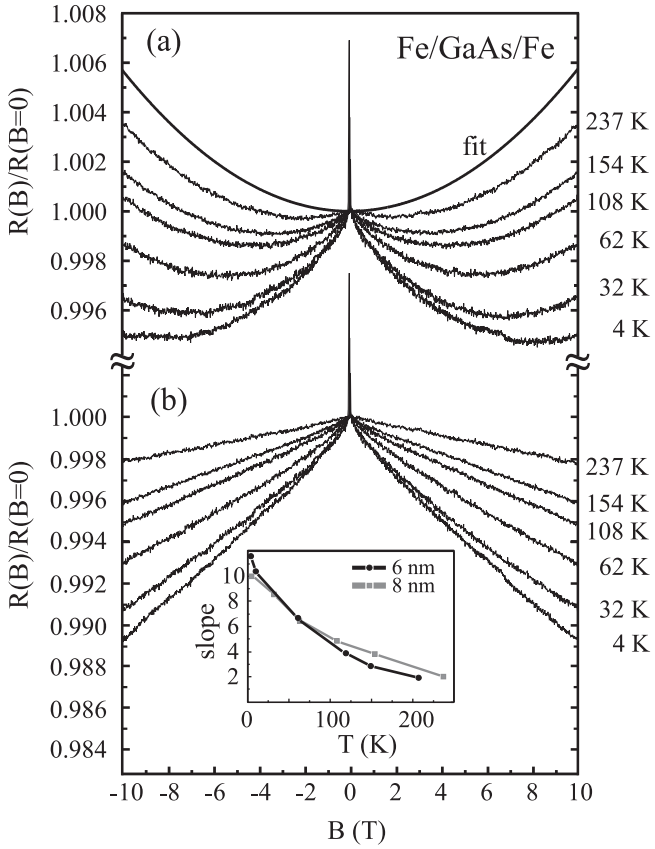

Figure 9. (a) Normalized resistance of an Fe/GaAs(001)/Fe junction with $d = 8$ nm as a function of temperature. The fit of the positive MR contribution is obtained by taking the difference between the 237 K trace and a line with slope $\mathrm{d}R(237\ \mathrm{K})/\mathrm{d}B$ taken close to $B = 0$ outside the TMR regime. (b) After subtraction of the T-independent positive MR contribution ('fit') from all traces in (a) a linear negative MR is obtained. The temperature dependence of the slope of the linear MR is shown in the inset for samples with 6 and 8 nm barrier thickness.

the raw data, showing a gradual increase of positive MR with increasing temperature. We then subtract from each trace the temperature-independent contribution, denoted as 'fit' in figure 9(a). We approximated this contribution by subtracting a linear contribution with slope $\mathrm{d}R(B, 237\ \mathrm{K})/\mathrm{d}B|_{B\sim 0}$ from the $R(B, 237\ \mathrm{K})$ trace. Subtracting the resulting 'fit' from the raw data gives a linear negative MR displayed in figure 9(b) for the investigated temperature range. The slope of the negative MR as a function of temperature is shown for two samples in the inset of figure 9(b). Though the detailed mechanism is not yet clear, we ascribe this negative MR to the spin polarization of the tunnelling current.

Possible mechanisms to explain the linear negative MR involve (i) spin-dependent barrier heights due to the Zeeman effect or (ii) suppression of spin-flip scattering at the interface and at magnetic impurities in the barrier with increasing magnetic field.

Concerning point (i): the spin splitting of the conduction band edge should cause different tunnelling barriers for spin-up and spin-down electrons. However, the observed temperature dependence of $\Delta\sigma/\sigma$ cannot be explained in this picture. The estimated size of the magnetoresistance change due to a spin-split conduction band is significantly smaller than

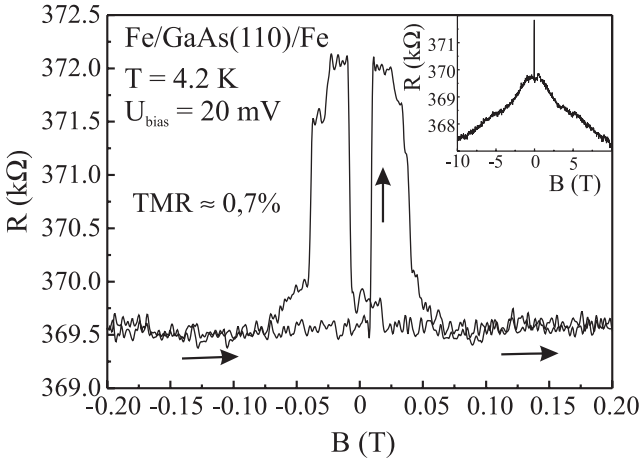

Figure 10. TMR traces for an Fe/GaAs(110)/Fe tunnel junction with $d = 10$ nm at 4.2 K. The inset shows the high-field magnetoresistance. The applied bias voltage was 20 mV in both cases.

observed in experiment [18]. Furthermore, the sign of the MR effect would be in conflict with recent experiments claiming that the tunnelling current is carried by the iron's majority spins, i.e. by spins which are aligned antiparallel to the applied magnetic field [19]. Since the g-factor in GaAs is negative the tunnelling barrier increases for spin-down electrons (antiparallel to the applied field) while getting lowered for spin-up electrons. Contrary to our experimental observation, this should cause a linearly increasing MR.

Spin-flip scattering (ii) at the interface or in the barrier, on the other hand, might be an alternative source of the negative MR. The diffusion of iron 'dopes' the thin GaAs membrane with potential spin-flip scatterers. This effect can explain the experimental results of a decreasing resistance with an increasing magnetic field qualitatively. A more detailed analysis of the negative MR can be found in [18].

In order to check the dependence of the TMR on the surface of the tunnelling barrier, we made experiments with GaAs(110) barriers. In contrast to GaAs(001), the surface of GaAs(110) is nonpolar. A charge transfer from the Ga to As atoms results in fully filled As dangling bonds and completely empty Ga dangling bonds. Consequently this results in a charge neutral surface, which should be chemically more stable. The preparation of the (110) barrier is the same as illustrated above. Figure 10(a) shows the tunnelling magnetoresistance of a 10 nm thick GaAs(110) barrier sandwiched between two iron films with 4 and 20 nm thickness. The TMR effect is about 0.7% and therefore even smaller than for the (001) barriers. In addition, the negative high-field MR seems to be even more pronounced for the (110) orientation (figure 10(b)). These measurements suggest that using the nonpolar (110) surface for tunnelling barriers cannot enhance the TMR effect.

4. Conclusion

In summary, we have demonstrated that quantum mechanical tunnelling is the dominant transport mechanism through epitaxial GaAs barriers. We see a pronounced tunnelling magnetoresistance effect in Fe/GaAs/Fe elements which can be drastically decreased by annealing. This indicates the sensitivity of the TMR effect to layer intermixing. The maximum spin polarization extracted from these experiments was about 10%, suggesting that a significant

amount of spin polarization (compared to bulk iron) is lost by scattering or that tunnelling is dominated by interface states with different spin polarization. Moreover, we have observed a linear negative high-field MR. This negative MR contribution is only observed for the ferromagnetic iron contacts and is absent if iron is replaced by copper or gold electrodes. Simple models like spin-dependent tunnelling barriers and spin-flip scattering in the barrier were suggested as explanations. TMR measurements on nonpolar GaAs(110) barriers showed no improvement compared to results obtained on polar GaAs(001) barriers.

Acknowledgments

Financial support by the BMBF (grant 01BM921) and by the DFG (Forschergruppe 370) is gratefully acknowledged. TD's research in Germany is supported by the Alexander von Humboldt foundation. The authors like to thank Gerrit Bauer, Jens Siewert and Wulf Wulfhekel for valuable discussions.

References

[1] Daughton J M 1997 *J. Appl. Phys.* **81** 3758
Gallagher W J, Kaufman J H, Parkin S S P and Scheuerlin R E 1997 *US Patent Specification* No. 5 640 343
[2] Moodera J S, Kinder L R, Wong T M and Meservey R 1995 *Phys. Rev. Lett.* **74** 3273
[3] Tsunoda M, Nishikawa K, Ogata S and Takahashi M 2002 *Appl. Phys. Lett.* **80** 3135
[4] MacLaren J M, Butler W H and Zhang X-G 1998 *J. Appl. Phys.* **83** 6521
[5] Mavropoulos P, Wunnicke O and Dederichs P H 2002 *Phys. Rev.* B **66** 024416
[6] Mosca D H, George J M, Maurice J L, Fert A, Eddrief M and Etgens V H 2001 *J. Magn. Magn. Mater.* **226–230** 917
[7] Gustavsson F, George J-M, Etgens V H and Eddrief M 2001 *Phys. Rev.* B **64** 184422/1
[8] Jonker B T 2003 *Proc. IEEE* **91** 727
[9] Kreuzer S, Wegscheider W and Weiss D 2001 *J. Appl. Phys.* **89** 6751
[10] Kreuzer S, Moser J, Wegscheider W, Weiss D, Bichler M and Schuh D 2002 *Appl. Phys. Lett.* **80** 4582
[11] Mavropoulos P, Papanikolaou N and Dederichs P H 2000 *Phys. Rev. Lett.* **85** 1088
[12] Madelung O 1996 *Semiconductors—Basic Data* 2nd edn (Berlin: Springer)
[13] Simmons J G 1963 *J. Appl. Phys.* **34** 1793
[14] Jullière M 1975 *Phys. Lett.* **54A** 225
[15] Hanbicki A T, Jonker B T, Itskos G, Kioseoglou G and Petrou A 2002 *Appl. Phys. Lett.* **80** 1240
[16] Hanbicki A T, van 't Erve O M J, Magno R, Kioseoglou G, Li C H, Jonker B T, Itskos G, Mallory R, Yasar M and Petrou A 2003 *Appl. Phys. Lett.* **82** 4092
[17] Eaves L, Stevens K W H and Sheard F W 1986 *The Physics and Fabrication of Microstructures and Microdevices* ed M J Kelly and C Weisbuch (Berlin: Springer) p 343
[18] Zenger M, Moser J, Wegscheider W, Weiss D and Dietl T 2004 *J. Appl. Phys.*
(Zenger M, Moser J, Wegscheider W, Weiss D and Dietl T 2004 *Preprint* cond-mat/0404351)
[19] Jonker B T, Hanbicki A T, Pierce D T and Stiles M D 2003 *Preprint* cond-mat/0304457